Original Article

Enzalutamide-resistant related lncRNA NONHSAT210528 promotes the proliferation and invasion of prostate cancer

Chen Ye[1#], Yuan-Gui Chen[1#], Sheng-Fei Qin[1], Shou-Yan Tang[1], Song Li[1], Min-Feng Shi[2], Tie Zhou[3]

[1]Department of Urology, Shanghai Changhai Hospital, Shanghai, China; [2]Reproduction Center, Shanghai Changhai Hospital, Shanghai, China; [3]Department of Urology, Shanghai Fourth People's Hospital, School of Medicine, Tongji University, Shanghai, China

Contributions: (I) Conception and design: C Ye, T Zhou; (II) Administrative support: MF Shi, T Zhou; (III) Provision of study materials or patients: YG Chen, SF Qin; (IV) Collection and assembly of data: MF Shi; (V) Data analysis and interpretation: SY Tang, S Li; (VI) Manuscript writing: All authors; (VII) Final approval of manuscript: All authors.

[#]These authors contributed equally to this work.

Correspondence to: Tie Zhou. No. 1279 Sanmen Road, Shanghai 200434, China. Email: wenzhoutie@163.com; Min-Feng Shi. 168 Changhai Road, Shanghai 200433, China. Email: minfengshi@163.com.

Background: As a new-generation androgen-receptor antagonist, enzalutamide is a first-choice drug for advanced prostate cancer (PCa) patients. However, secondary resistance to enzalutamide poses a new challenge in the treatment of cancer. Long non-coding RNA (lncRNA) regulates cell function through many levels and mechanisms, and also plays an important role in the biological behaviors of tumors.

Methods: LncRNA microarrays were used to detect enzalutamide-resistant related lncRNA in enzalutamide-resistant C4-2 (C4-2 ENZ-R) cells and corresponding parent cells. Cell Counting Kit 8, flow cytometry, and transwell assays were used to test the effect of lncRNA NONHSAT210528 on the function of PCa cells. RNA pulls down and the luciferase report gene was used to detect the competitive endogenous RNA (ceRNA) mechanism. The culture supernatant of C4-2 and C4-2b cells was transferred to the lower chamber for transwell assay of human umbilical endothelial cells (HUVECs).

Results: The lncRNA microarray analysis showed that there were significant differences in the expression of many lncRNAs between the C4-2 ENZ-R and C4-2 cells. The real-time polymerase chain reaction (PCR) detection showed that the expression of lncRNA NONHSAT210528 was significantly higher in the C4-2 ENZ-R cells than the C4-2 cells. The Transwell assays showed that lncRNA NONHSAT210528 overexpression increased the invasion of the C4-2 and C4-2b cells. The cell-wound scratch and the transwell assays showed that the culture supernatant of C4-2 and C4-2b cells with overexpressed lncRNA NONHSAT210528 promoted the migration and invasion of HUVECs. Furthermore, lncRNA NONHSAT210528 regulated the expression of YOD1 dependent on miR-21.

Conclusions: Enzalutamide-resistant related lncRNA NONHSAT210528 appears to promote the proliferation and invasion of PCa cells by functioning as a ceRNA and regulating the miR-21-5p/YOD1 signal pathway.

Keywords: Enzalutamide; long non-coding RNA (lncRNA); miRNA; YOD1; prostate cancer (PCa)

Submitted Dec 31, 2021. Accepted for publication Apr 28, 2022.

doi: 10.21037/tau-22-99

View this article at: https://dx.doi.org/10.21037/tau-22-99

Introduction

Prostate cancer (PCa) is the second most common cancer in the world, and is also a leading cause of cancer-related death in men (1,2). In recent years, the incidence rate of PCa has increased significantly in China, and the proportion of patients with advanced PCa in China is much higher than that in European and American countries (3). Androgen

deprivation is the main treatment for patients with advanced PCa. As a new-generation androgen-receptor antagonist, enzalutamide effectively prolongs the overall survival of patients, and is a first-choice drug for metastatic castration resistant PCa (mCRPC) patients (4). However, 20–40% of patients with mCRPC patients demonstrate de novo resistance to enzalutamide, and most patients will acquire drug resistance after 1–2 years of treatment sensitivity (5-7). After secondary resistance, the disease develops rapidly and maliciously, and patient prognosis is poor (5-7). Thus, enzalutamide-resisant molecular regulatory mechanism needs to be studied urgently, and the corresponding early warning markers and intervention targets identified.

Long non-coding RNA (lncRNA) is a class of non-coding RNA molecules with a length >200 nt (8-10). LncRNA regulates cell function through many levels and mechanisms, including chromatin modification, transcriptional regulation, and microRNA function regulation, and it also plays an important role in the biological behavior of tumors (11,12). For example, lncRNA SChLAP1 enhances the ability of invasion and metastasis of PCa by inhibiting the function of the SWItch/Sucrose Non-Fermentable complex (13). ROR1-HER3 and the Hippo-YAP pathway depend on lncRNA MAYAY mediated crosstalk activation to induce osteoclast differentiation and promote bone metastasis in breast cancer (14). LncRNA TTTY15 from the Y chromosome upregulates the expression of cell division protein kinase 6 and fibronectin-1 through the sponge adsorption of miRNA-let-7, which promotes the progression of PCa (15). However, there are few reports about the role of lncRNA in disease progression after enzalutamide resistance in PCa.

In this study, we found that enzalutamide resistance induced by lncRNA NONHSAT210528 promoted the expression of YOD1 through the mechanism of competitive endogenous RNA (ceRNA) by regulating the expression of miR-21-5p in PCa cells after resistance to enzalutamide. Overall, lncRNA NONHSAT210528 directly enhanced the malignant characteristics of PCa cells. We present the following article in accordance with the ARRIVE reporting checklist (available at https://tau.amegroups.com/article/view/10.21037/tau-22-99/rc).

Methods

LncRNA expression analysis

The total RNA of the samples was quantified by NanoDrop ND-2000 (Thermo Scientific, USA), and RNA integrity was detected by Agilent Bioalyzer 2100 (Agile technologies, USA). After the RNA quality inspection was qualified, the sample marking, chip hybridization and elution refer to the standard flow of chip. First, the total RNA was reverse transcribed into double-stranded complementary DNA (cDNA), and the cDNA labeled with cyanine-3-CTP (Cy3) was then synthesized. The labeled cDNA was hybridized with microarray, and the original image was obtained using the Agilent scanner G2505C (Agilent Technologies) after elution. The original data were extracted using Feature Extraction software (Version 10.7.1.1, Agilent Technologies). Next, quantitative standardization and the subsequent processing were carried out using geneprinting software (version 13.1, Agilent technologies). The standardized data were filtered, and at least 1 group of 100% labeled "P" probes in each group of samples were left for the subsequent comparative analysis. Differential genes and differential lncRNAs were screened by the P value and the fold-change value of the *t*-test. The screening criteria were an upregulated or downregulated fold-change value ≥2.0 and P value ≤0.05.

Cell culture, lncRNA NONHSAT210528 overexpression and knockdown

Human PCa cell lines (C4-2, C4-2b) were purchased from American Type Culture Collection (ATCC). All PCa cells were cultured in RPMI 1640 medium supplemented with 10% Fetal bovine serum at 37 ℃ in 5% CO_2. Enzalutamide-resistant C4-2 cell (C4-2 ENZ-R) was established by being exposed to increasing concentrations of enzalutamide according to previous study (16). For NONHSAT210528 overexpression, we cloned NONHSAT210528 into pLVX-vector by gene synthesis and NONHSAT210528 overexpression vector (pLVX-NONHSAT210528) was transferred into cells. The siRNA target sequences (5'-ACCCACTATAATGTATCATTAGT-3') were used for knockdown NONHSAT210528, and were cloned into pLKO.1-Vector.

Real-time PCR analysis

Total RNA was extracted from the cells and tissue by Trizol reagent, and the concentration of RNA was detected by NanoDrop. One microgram of extracted RNA was reverse transcribed using an RNA reverse transcription kit. A real-time fluorescent quantitative polymerase chain reaction

(PCR) was performed using the SYBR Green Real-Time Quantitative PCR Master Mix kit, and the sample was added according to the instructions of the kit. The reaction conditions were as follows: Procedure 1: 95 ℃, 30 s, 1 cycle; Program 2: 95 ℃, 5 s, 50 cycles, 60 ℃, 34 s; Program 3: 95 ℃, 5 s, 1 cycle, 65 ℃, 60 s, 97 ℃, 1 s, and Program 4: 42 ℃, 30 s, 1 cycle. The relative gene expression was calculated by the $2^{-\Delta\Delta CT}$ method, and the messenger RNA (mRNA) expression was corrected by glyceraldehyde 3-phosphate dehydrogenase expression, and the lncRNA expression was corrected by GAPDH expression.

CCK-8 and colony formation assays

The cells were seeded into a 96-well culture plate with a density of 4,000 cells/well. The activity of cells was detected using Cell Counting Kit-8 (CCK-8) at 24 h, 36 h, 48 h, and 96 h after inoculation with 10 μL of CCK-8 in a 37 ℃ incubator for 2 h. The absorbance at 450 nm was detected by an enzyme reader. For the colony formation assay, cells were plated in 6-well plates (1,500 cells/well). After incubation for seven days, the cells were fixed with paraformaldehyde and stained with crystal violet stain.

RNA pull down

The MS2bs sequence was coupled to the lncRNA NONHSAT210528 sequence, lncRNA NONHSAT210528 overexpression vector coupled with MS2Bs sequence was transfected into cells. The cells were lysed and incubated with MS2 protein labeled by magnetic beads with cell lysate, and then the pull down product was detected by qPCR. Biotin labeled miRNA was incubated with cell lysate to form RNA-RNA complex. The complex can be combined with streptavidin labeled magnetic beads to separate from other components in the incubation solution. The complex was eluted and detected by qPCR.

Transwell and wound scratch assay

After 1:1 mixing of Dulbecco's Modified Eagle Medium and matrigel, 50 μL of the liquid was evenly spread in the Transwell upper chamber and placed in a 37 ℃ incubator for 45 min. The cells were seeded into the Transwell upper chamber at a density of 20,000 cells/well; the Transwell upper chamber contained serum-free medium, while 700 μL of a medium containing 5% serum was added to the lower chamber. The cells at the bottom of the Transwell chambers were stained with crystal violet and counted after photographs had been taken. To perform the wound scratch assay, cells were seeded on 6-well plates and transfected for 48 h, followed by the creation of an artificial, homogenous scratch wound on a confluent monolayer culture of cells with a pipette tip. The cells were imaged at 2 different time points (0 and 24 h).

Western blot analysis

After the culture supernatant was sucked off, it was washed once with phosphate buffer, and 100 μL of RIPA lysate containing 1 mmol/L of PMSF was added to each hole. The cells were scraped off on ice with a cell scraper, lysed on ice for 30 min, centrifuged at 12,000 r/min for 15 min at 4 ℃, and the protein lysate supernatant was then collected. The bicinchoninic acid assay method was used to detect the protein concentration. 10% sodium dodecyl-sulfate polyacrylamide gel electrophoresis was prepared, and 20 μg of protein was added to each hole. After electrophoresis, the protein was transferred to polyvinylidene fluoride membranes at 300 Ma for 120 min, sealed with 5% BSA for 1 h, incubated with primary antibody at 4 ℃ overnight, washed with Tris Buffered Saline with Tween (TBST) 3 times, incubated with secondary antibody at room temperature for 1 h, washed with TBST another 3 times, and then developed with ECL developer.

Tumor xenograft assay

Experiments were performed under a project license (No. 2019QN02) granted by Animal Care and Use Committee of Shanghai Changhai Hospital, the First Affiliated Hospital of Naval Military Medical University, in compliance with eighth edition guidelines for the care and use of experimental animals (17). A protocol was prepared before the study without registration. Male nude mice (BALB/C, 6 weeks old) were purchased from Shanghai Laboratory Animal Center (SLAC, China) and housed under specific pathogen-free conditions. The mice were divided randomly into four groups (five mice per group): (I) pLVX-NONHSAT210528 group; (II) pLVX-Vector group; (III) pLKO.1- NONHSAT210528 group; (IV) pLKO.1-Vetor group. After digesting the logarithmic growth C4-2 cells with trypsin, the C4-2 cells were resuspended with serum-free medium, and the cell concentration was adjusted to 1.0×10^7 cells/mL. Next, 100 μL of cell suspension was injected into the back of the male nude mice. The tumor

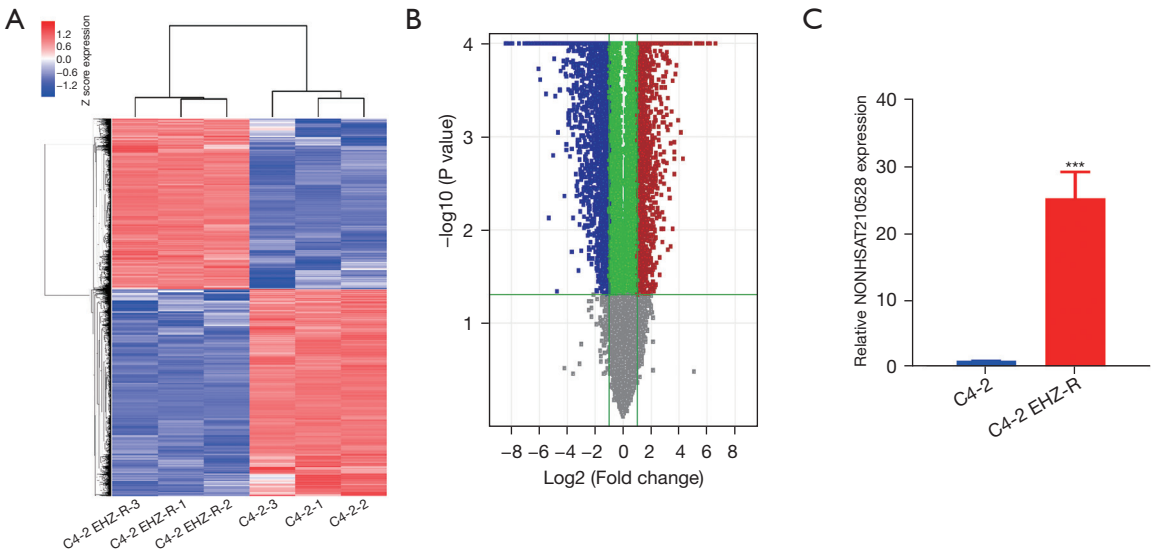

Figure 1 LncRNA NONHSAT210528 was upregulated in enzalutamide-resistant C4-2 cells. (A) Heat map showing the different expression of lncRNA in C4-2 cells and enzalutamide-resistant C4-2 (C4-2 ENZ-R) cells. (B) Volcano plot showing the different expressions of lncRNA in C4-2 cells and C4-2 ENZ-R cells. (C) Real-time PCR detection showing the expression of lncRNA NONHSAT210528 in C4-2 and C4-2 ENZ-R cells. ***, P<0.001 compared to the C4-2 group. lncRNA, long non-coding RNA; PCR, polymerase chain reaction.

volume was measured once a week. After the sixth week of inoculation, the mice were killed by cervical dislocation. The tumor tissue was removed, weighed, and photographed. The animal experiment was done in the Laboratory Animal Centre of Naval Military Medical University.

Statistical analysis

SPSS analysis software (SPSS 22.0) was used for the statistical analysis. The results are expressed as the mean ± standard deviation. The means of 2 samples were compared by an independent sample *t* test, and the means of multiple samples were compared by a one-way analysis of variance. A P value <0.05 was considered statistically significant.

Results

LncRNA NONHSAT210528 was upregulated in enzalutamide-resistant C4-2 cells

Enzalutamide resistance is the reason for the failure of enzalutamide treatment. Thus, it is necessary to explore the specific molecular mechanism underlying enzalutamide resistance. We constructed an enzalutamide-resistant cell line C4-2 ENZ-R *in vitro*, and analyzed expression differences in lncRNA between C4-2 ENZ-R and its parent cell line C4-2 using lncRNA microarrays. The lncRNA microarray analysis showed that there were significant differences in the expression of many lncRNAs between the C4-2 ENZ-R and C4-2 cells. Notably, 924 lncRNAs were downregulated, and 694 lncRNAs were upregulated in the C4-2 ENZ-R cells compared to the C4-2 cells (see *Figure 1A*,*1B*). The real-time PCR detection showed that the expression of lncRNA NONHSAT210528 was significantly higher in the C4-2 ENZ-R cells than in the C4-2 cells (see *Figure 1C*).

LncRNA NONHSAT210528 knockdown suppressed the proliferation and invasion of the C4-2 and C4-2b cells

To detect the effect of lncRNA NONHSAT210528 on the function of PCa cells, we constructed a short-harpin RNA (shRNA) specific target for lncRNA NONHSAT210528. The real-time PCR detection results showed that the expression of lncRNA NONHSAT210528 was significantly more downregulated in the pLKO.1-NONHSAT210528 group than the pLKO.1-vector group in the C4-2 and C4-2b cells (see *Figure 2A*). The CCK-8 detection results showed that the cell viability of the C4-2 and C4-2b cells was lower in the pLKO.1-NONHSAT210528 group than the pLKO.1-vector group at 48, 72, and 96 h (see *Figure 2B*). The cell-cycle detection results showed that lncRNA

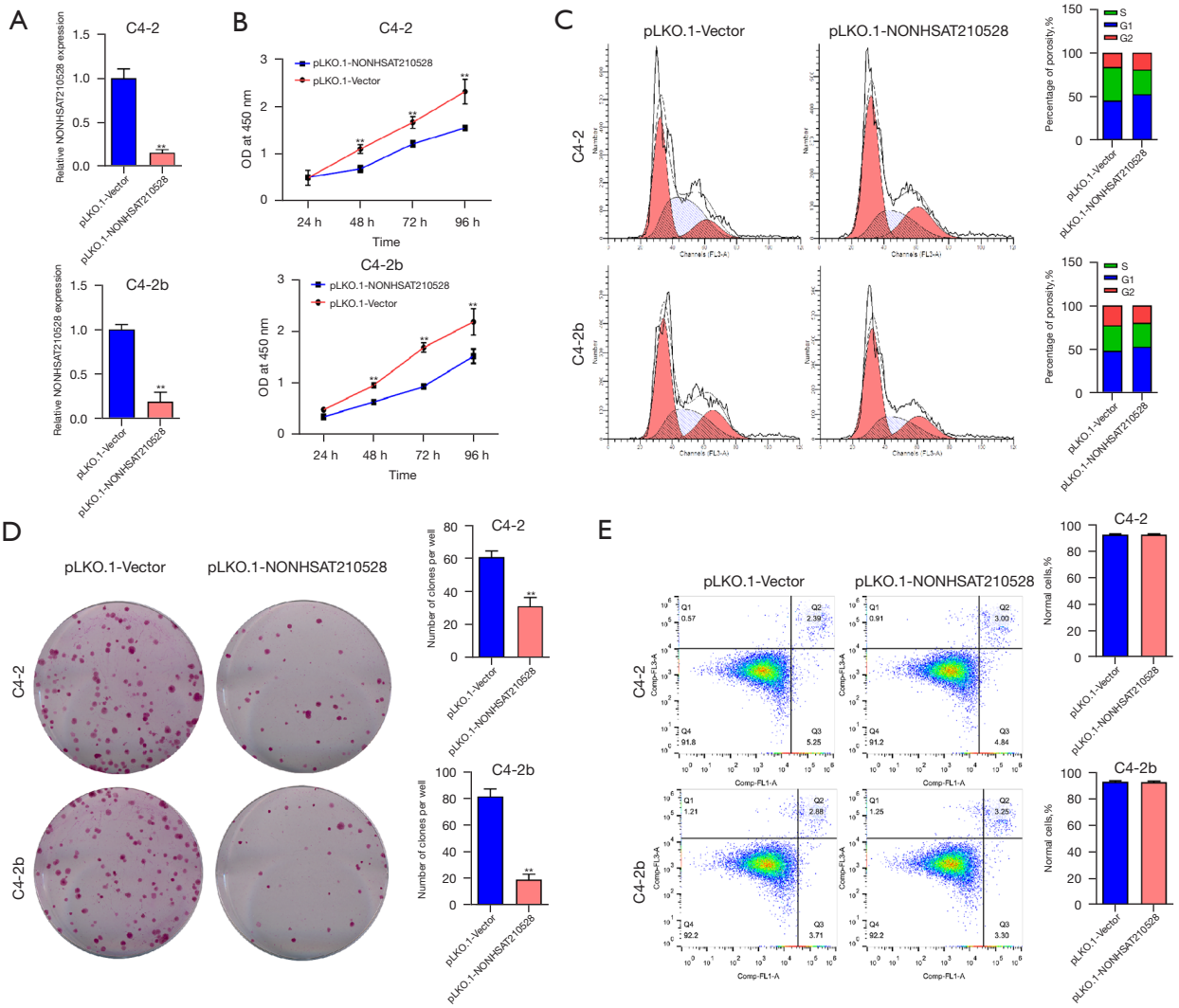

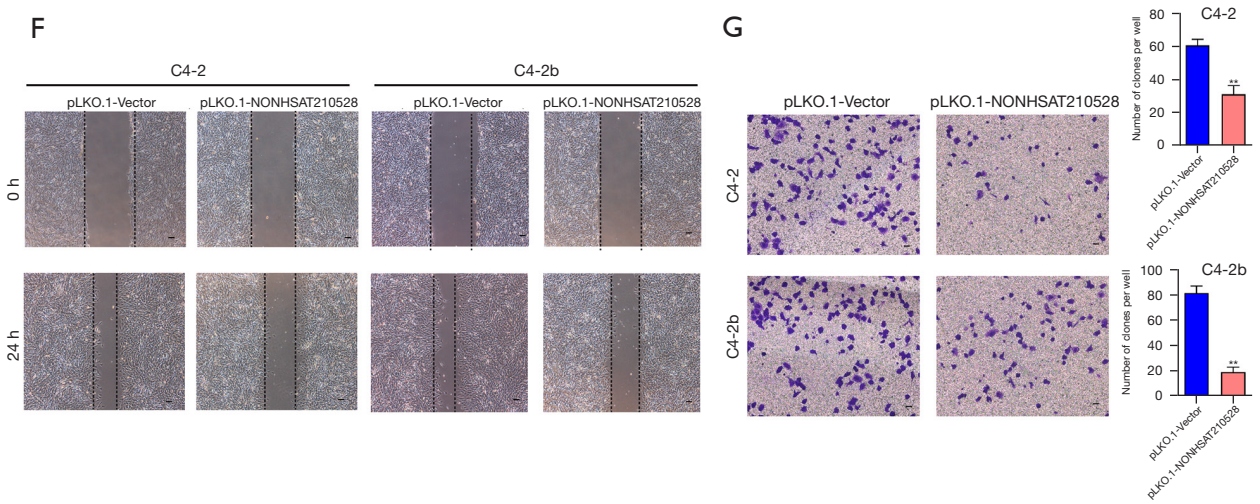

Figure 2 LncRNA NONHSAT210528 knockdown suppressed the proliferation and invasion of C4-2 and C4-2b cells. (A) Real-time PCR detected the expression of lncRNA NONHSAT210528 in C4-2 and C4-2b cells with lncRNA NONHSAT210528 knockdown. (B) CCK-8 detected the proliferation of C4-2 and C4-2b cells with lncRNA NONHSAT210528 knockdown. (C) Flow cytometry detected the cell cycle of C4-2 and C4-2b cells with lncRNA NONHSAT210528 knockdown. (D) Clone formation detected the proliferation of C4-2 and C4-2b cells with lncRNA NONHSAT210528 knockdown. The cells were stained with crystal violet stain. (E) Flow cytometry detected the apoptosis of C4-2 and C4-2b cells with lncRNA NONHSAT210528 knockdown. (F) Cell-wound scratch assays detected the migration of C4-2 and C4-2b cells with lncRNA NONHSAT210528 knockdown. The cells were imaged at same position of 6-well plates at 2 different time points (0 and 24 h). Scale bar, 100 μm. (G) Transwell assays detected the invasion of C4-2 and C4-2b cells with lncRNA NONHSAT210528 knockdown. The cells at the bottom of the Transwell chambers were stained with crystal violet. Scale bar, 100 μm. **, P<0.01 compared to the pLKO.1-Vector group. OD, optical density; lncRNA, long non-coding RNA; PCR, polymerase chain reaction.

NONHSAT210528 knockdown increased the proportion of the G1 and reduced the proportion of the G2 and S phase (see *Figure 2C*). The clone formation detection results showed that lncRNA NONHSAT210528 knockdown reduced the number of clones in the C4-2 and C4-2b cells (see *Figure 2D*). The flow cytometry detection results showed that lncRNA NONHSAT210528 knockdown had no effect on the apoptosis of the C4-2 and C4-2b cells (see *Figure 2E*). The cell-wound scratch assays showed that lncRNA NONHSAT210528 knockdown reduced the migration of the C4-2 and C4-2b cells (see *Figure 2F*). The Transwell assays showed that lncRNA NONHSAT210528 knockdown reduced the invasion of the C4-2 and C4-2b cells (see *Figure 2G*).

LncRNA NONHSAT210528 overexpression promoted the proliferation and invasion of the C4-2 and C4-2b cells

To detect the effect of lncRNA NONHSAT210528 on the function of PCa cells, we constructed a lentiviral vector to overexpress lncRNA NONHSAT210528. The real-time PCR detection results showed that the expression of lncRNA NONHSAT210528 was significantly more upregulated in the pLVX-NONHSAT210528 group than the pLVX-vector group in the C4-2 and C4-2b cells (see *Figure 3A*). The CCK-8 detection results showed that the cell viability of the C4-2 and C4-2b cells was higher in the pLVX-NONHSAT210528 group than the pLVX-vector group at 48, 72, and 96 h (see *Figure 3B*). The cell-cycle detection results showed that lncRNA NONHSAT210528 overexpression decreased the proportion of G1 and increased the proportion of the G2 and S phase (see *Figure 3C*). The clone formation detection results showed that lncRNA NONHSAT210528 overexpression increased the number of clones in the C4-2 and C4-2b cells (see *Figure 3D*). The flow cytometry detection results showed that lncRNA NONHSAT210528 overexpression had no effect on the apoptosis of the C4-2 and C4-2b cells (see *Figure 3E*). The cell-wound scratch assays showed that lncRNA NONHSAT210528 overexpression increased the migration of the C4-2 and C4-2b cells (see *Figure 3F*). The Transwell assays showed that lncRNA NONHSAT210528 overexpression increased the invasion of the C4-2 and C4-

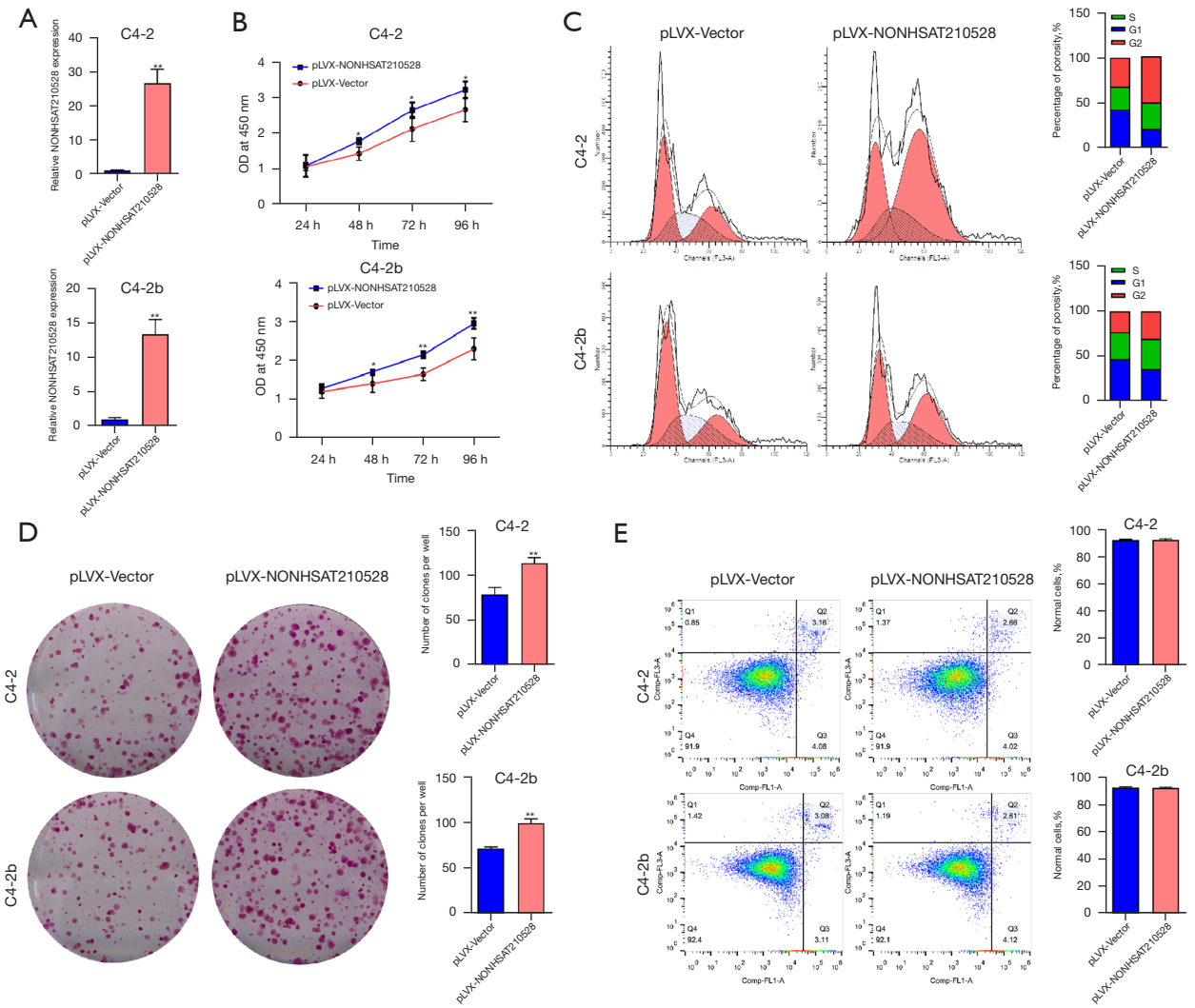

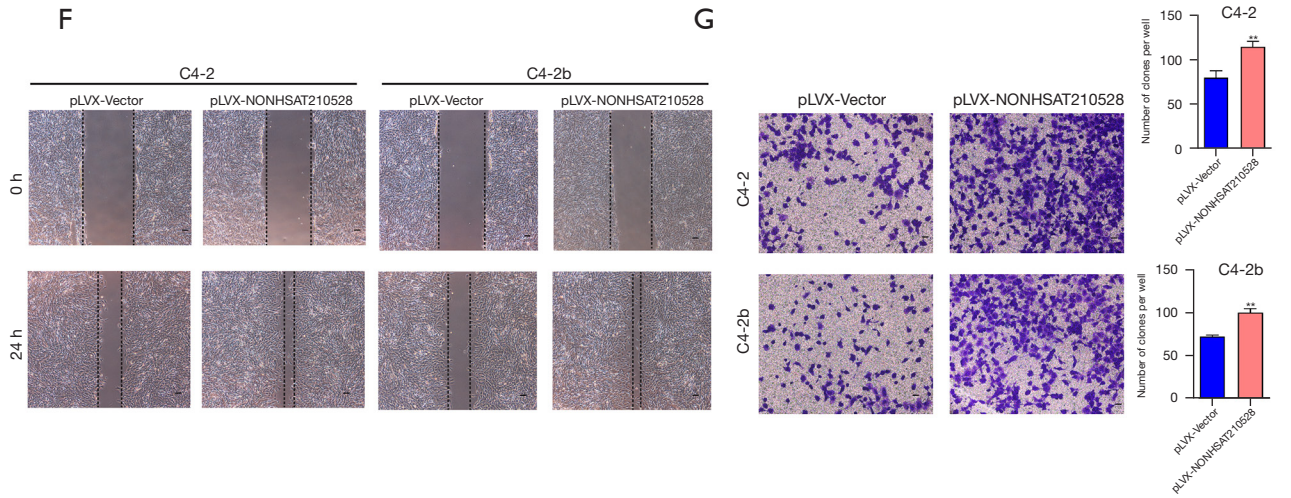

Figure 3 LncRNA NONHSAT210528 overexpression promoted the proliferation and invasion of C4-2 and C4-2b cells. (A) Real-time PCR detected the expression of lncRNA NONHSAT210528 in C4-2 and C4-2b cells with lncRNA NONHSAT210528 overexpression. (B) CCK-8 detected the proliferation of C4-2 and C4-2b cells with lncRNA NONHSAT210528 overexpression. (C) Flow cytometry detected the cell cycle of C4-2 and C4-2b cells with lncRNA NONHSAT210528 overexpression. (D) Clone formation detected the proliferation of C4-2 and C4-2b cells with lncRNA NONHSAT210528 overexpression. The cells were stained with crystal violet stain. (E) Flow cytometry detected the apoptosis of C4-2 and C4-2b cells with lncRNA NONHSAT210528 overexpression. (F) Cell-wound scratch assays detected the migration of C4-2 and C4-2b cells with lncRNA NONHSAT210528 overexpression. The cells were imaged at same position of 6-well plates at 2 different time points (0 and 24 h). Scale bar, 100 μm. (G) Transwell assays detected the invasion of C4-2 and C4-2b cells with lncRNA NONHSAT210528 overexpression. The cells at the bottom of the Transwell chambers were stained with crystal violet. Scale bar, 100 μm. *, P<0.05, **, P<0.01 compared to the pLKO.1-Vector group. OD, optical density; lncRNA, long non-coding RNA; PCR, polymerase chain reaction.

2b cells (see *Figure 3G*).

LncRNA NONHSAT210528 regulated the proliferation of C4-2 cells in vivo

To detect the effect of lncRNA NONHSAT210528 on the proliferation of the C4-2 cells *in vivo*, we constructed a subcutaneous ectopic tumor formation model. The detection results showed that the overexpression of lncRNA NONHSAT210528 promoted the proliferation and that lncRNA NONHSAT210528 knockdown reduced the proliferation of C4-2 cells *in vivo* (see *Figure 4A*). The pLVX- NONHSAT210528 group had a higher weight and volume than the pLVX-vector group, and the pLKO.1-NONHSAT210528 group had a lower weight and volume than the pLKO.1-vector group (see *Figure 4B,4C*).

LncRNA NONHSAT210528 regulated the epithelial-mesenchymal transformation (EMT)-related gene in C4-2 and C4-2b cells

EMT is a biological process in which epithelial cells are transformed into cells with a mesenchymal phenotype through specific procedures. EMT is an important biological process by which malignant tumor cells derived from epithelial cells acquire the abilities of migration and invasion. We found that lncRNA NONHSAT210528 overexpression promoted the expression of ZEB1, Snail, and Fibronection and inhibited the expression of E-cadherin (see *Figure 5A-5D*). Conversely, lncRNA NONHSAT210528 knockdown reduced the expression of ZEB1, Snail, and Fibronection, and promoted the expression of E-cadherin (see *Figure 5A-5D*).

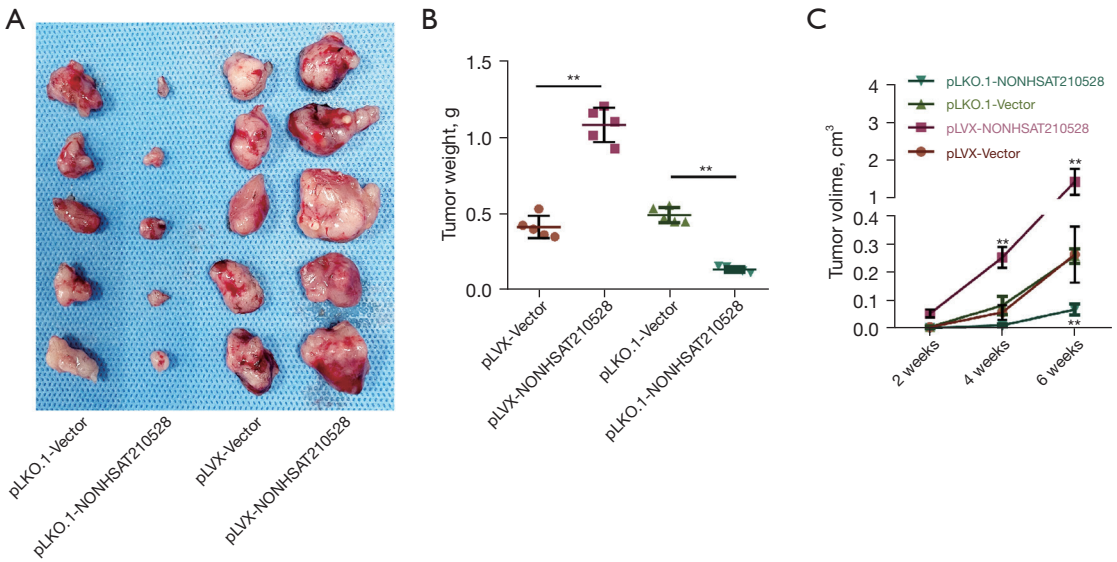

Figure 4 LncRNA NONHSAT210528 regulated the proliferation of C4-2 cells *in vivo*. (A) Picture showing the size of a subcutaneous ectopic tumor of a C4-2 cell with NONHSAT210528 overexpression or knockdown. (B) The tumor weight of a subcutaneous ectopic tumor of a C4-2 cell with NONHSAT210528 overexpression or knockdown. (C) The tumor volume of a subcutaneous ectopic tumor of a C4-2 cell with NONHSAT210528 overexpression or knockdown. **, P<0.01 compared to the control group. lncRNA, long non-coding RNA.

The culture supernatant of C4-2 and C4-2b cells with overexpressed lncRNA NONHSAT210528 promoted the angiogenesis of human umbilical endothelial cells (HUVECs)

The rapid proliferation of tumor cells leads to local ischemia and hypoxia, which directly stimulate angiogenesis. Additionally, hypoxia also causes a variety of tissue cells, especially tumor cells, to secrete angiogenic factors, and promotes endothelial cell proliferation and chemotactic endothelial cell migration. The cell-wound scratch and the transwell assays showed that the culture supernatant of C4-2 and C4-2b cells with overexpressed lncRNA NONHSAT210528 promoted the migration and invasion of HUVECs, and the culture supernatant of C4-2 and C4-2b cells with down-regulated lncRNA NONHSAT210528 inhibited the migration and invasion of HUVECs (see *Figure 6A-6C*). The enzyme-linked immunoassays (ELISAs) showed that lncRNA NONHSAT210528 overexpression increased vascular endothelial growth factor (VEGF) expression, and lncRNA NONHSAT210528 knockdown suppressed VEGF expression (see *Figure 6D*).

LncRNA NONHSAT210528 regulated the function of miR-21

CeRNA is a gene expression regulation mode, which is regulated by RNA through miRNA reaction elements. RNA pull down was used to detect the combination of miRNA and lncRNA NONHSAT210528. MS2bs-NONHSAT210528 RNA pull down showed that miR-527, miR-509, miR-562, and miR-21-5p were more enriched in the MS2bs-NONHSAT210528 group than MS2BS-Rluc group (see *Figure 7A*). Biotin-miR-21-5p RNA pull down showed that lncRNA NONHSAT210528 was more enriched in the Biotin-miR-21-5p group than Biotin-miR-NC group (see *Figure 7B*). The double-luciferase reporter gene assays showed that lncRNA NONHSAT210528 combined with miR-21-5p (see *Figure 7C*). Next, we examined the effect of miR-21-5p on the function of the C4-2 and C4-2b cells. miR-21-5p overexpression inhibited the cell viability of the C4-2 and C4-2b cells, and miR-21-5p knockdown promoted the cell viability of the C4-2 and C4-2b cells (see *Figure 7D*,*7E*). Conversely, miR-21-5p overexpression inhibited the cell invasion of the C4-2

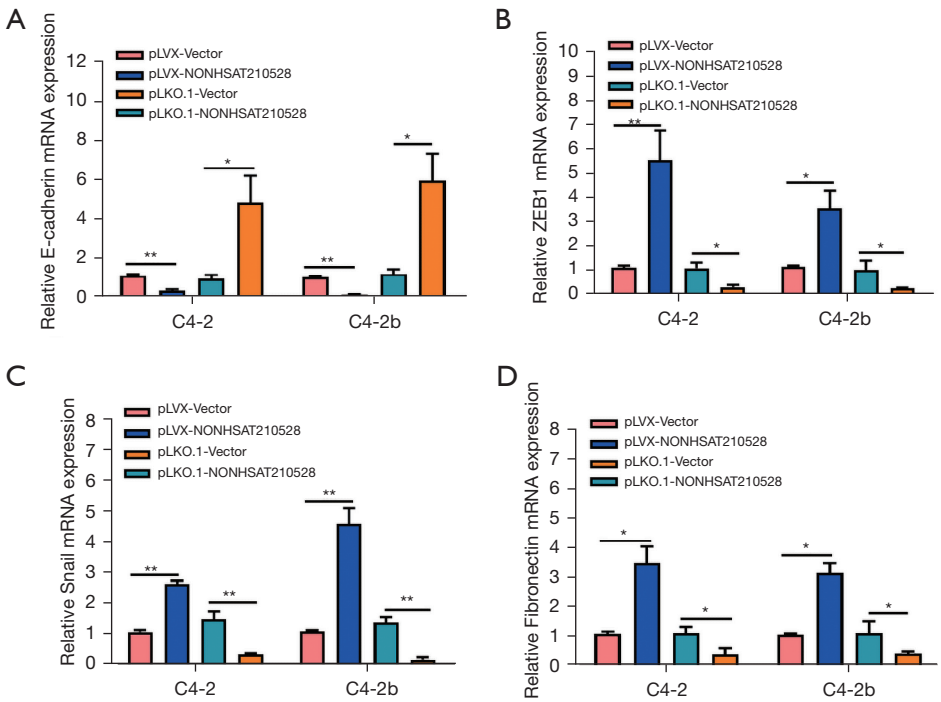

Figure 5 LncRNA NONHSAT210528 regulated the EMT-related gene in C4-2 and C4-2b cells. Real-time PCR detected the E-cadherin (A), ZEB1 (B), Snail (C) and Fibronectin (D) mRNA expression of C4-2 and C4-2b cells with NONHSAT210528 overexpression or knockdown. (A) Picture showing the size of a subcutaneous ectopic tumor of a C4-2 cell with NONHSAT210528 overexpression or knockdown. (B) The tumor weight of a subcutaneous ectopic tumor of a C4-2 cell with NONHSAT210528 overexpression or knockdown. (C) The tumor volume of a subcutaneous ectopic tumor of a C4-2 cell with NONHSAT210528 overexpression or knockdown. *, P<0.05; **, P<0.01 compared to the control group. lncRNA, long non-coding RNA; EMT, epithelial mesenchymal transition; PCR, polymerase chain reaction.

and C4-2b cells, and miR-21-5p knockdown promoted the cell invasion of the C4-2 and C4-2b cells (see *Figure 7F,7G*). However, the effect of lncRNA NONHSAT210528 on the invasion of the C4-2 and C4-2b cells was significantly reduced when the expression of miR-21-5p were inhibited (see *Figure 7H,7I*).

LncRNA NONHSAT210528 regulated the expression of YOD1 dependent on miR-21

Using the bioinformatics analysis software, we found that miR-21-5p targeted the 3'-untranslated region (3'-UTR) region of YOD1 mRNA. The real-time PCR results showed that miR-21-5p overexpression and knockdown did not affect the expression level of YOD1 mRNA (see *Figure 8A*). The double-luciferase reporter gene assay showed that the 3'-UTR region of YOD1 mRNA combined with miR-21-5p (see *Figure 8B*). The Western blot showed that miR-21-5p overexpression inhibited the expression of the YOD1 protein, while miR-21-5p knockdown promoted the expression of the YOD1 protein (see *Figure 8C*). Conversely, the overexpression of NONHSAT210528 promoted the expression of the YOD1 protein, but NONHSAT210528 did not promote the expression of YOD1 protein when miR-21-5p was knocked down (see *Figure 8D*).

Discussion

Docetaxel chemotherapy has been shown to increase the survival of CRPC patients to 18.9 months (18). The advent of the second-generation androgen-receptor antagonist of enzalutamide has innovated the new endocrine therapy concept of CRPC, and prolonged the median survival time of CRPC patients to 32.4 months (19). However, shortly after enzalutamide began to be widely used in clinical settings, new problems arose. About 42% of CRPC patients are not sensitive to

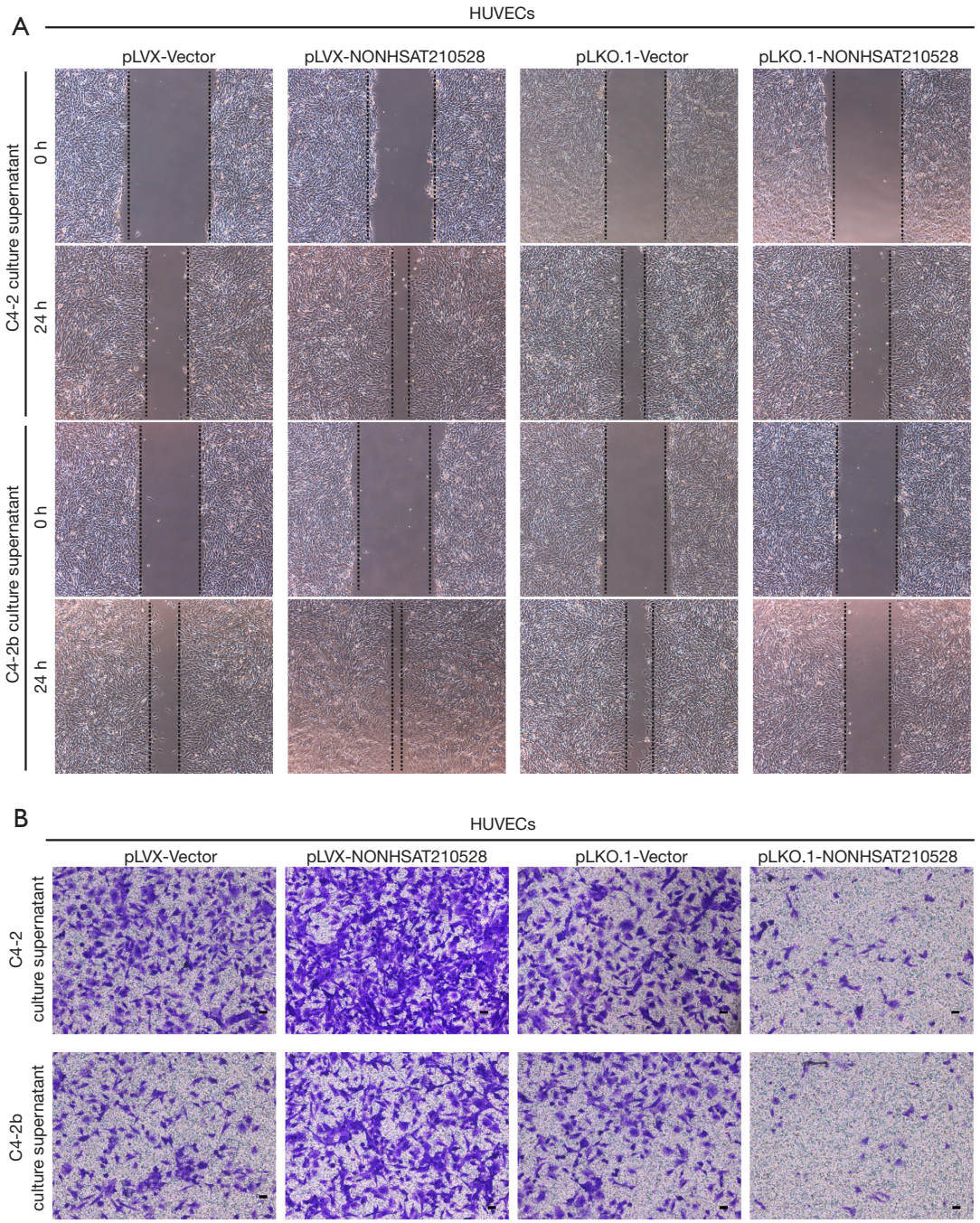

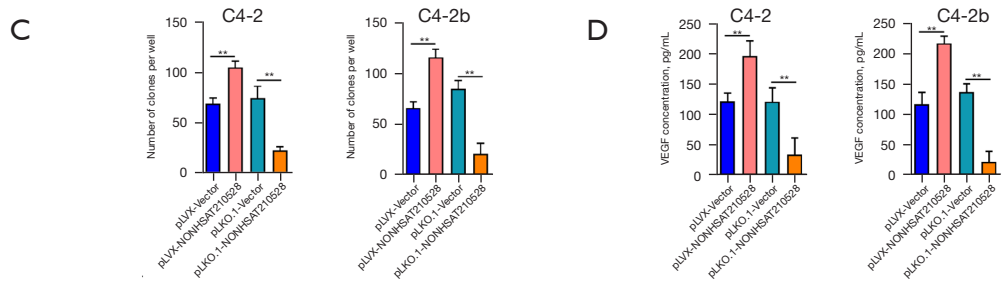

Figure 6 LncRNA NONHSAT210528 regulated the culture supernatant of C4-2 and C4-2b cells to induce the angiogenesis of HUVECs. (A) Cell-wound scratch assays detected the migration of HUVECs cultured with the cell culture supernatant of C4-2 and C4-2b cells with lncRNA NONHSAT210528 knockdown or overexpression. The cells were imaged at same position of 6-well plates at 2 different time points (0 and 24 h). Scale bar, 100 μm. (B) Transwell assays detected the invasion of HUVECs cultured with the cell culture supernatant of C4-2 and C4-2b cells with overexpressed or down-regulated lncRNA NONHSAT210528. The cells at the bottom of the Transwell chambers were stained with crystal violet. Scale bar, 100 μm. (C) Quantitative analysis of Transwell assays detected the invasion of HUVECs cultured with the cell culture supernatant of C4-2 and C4-2b cells with overexpressed or down-regulated lncRNA NONHSAT210528. (D) ELISA assays detected the VEGF expression in the cell culture supernatant of C4-2 and C4-2b cells with overexpressed or down-regulated lncRNA NONHSAT210528. Scale bar, 100 μm. **, P<0.01 compared to the control group. lncRNA, long non-coding RNA; HUVECs, human umbilical vein endothelial cells; VEGF, vascular endothelial growth factor.

enzalutamide treatment (20), and even if the treatment is effective, enzalutamide resistance will re-occur after 11.2 months (19). At present, the mechanism of enzalutamide resistance in PCa has not been clarified. Thus, exploring the molecular mechanism of enzalutamide resistance is very important to increase the sensitivity of enzalutamide treatment and prevent enzalutamide resistance. LncRNA is a kind of non-coding RNA with transcripts >200 nt. In recent years, developments in lncRNA research have shown that lncRNA plays an important role in tumor drug resistance (21). Thus, exploring the relationship between lncRNA and enzalutamide resistance in PCa has become a new molecular therapeutic target for PCa. In this study, we established enzalutamide-resistant C4-2 cells according to the method of previous study (16), then detecting the differential expression profiles of lncRNA between the parent cell line and enzalutamide-resistant cell line by lncRNA microarrays, to explore the molecular mechanism of lncRNA and enzalutamide resistance in PCa patients from a new perspective.

To date, most in-depth research on the related functions of lncRNA has focused on its role in cancer. Under normal physiological conditions, the expression of lncRNA is strictly regulated. Conversely, the abnormal expression of lncRNA is accompanied by the occurrence and development of many cancers. LncRNAs can not only promote tumor formation as protooncogenes, but also inhibit the proliferation and migration of tumor cells as tumor suppressor genes (22). The results of the lncRNA microarray analysis showed that the expression level of lncRNA NONHSAT210528 was significantly increased in the C4-2b-ENZR cells. The drug resistance of tumor cells to anti-cancer drugs is a main reason for the failure of chemotherapy (23,24). In both congenital and acquired drug resistance, the abnormal activation of the intracellular signal pathway is closely related to tumor drug resistance. LncRNAs can cause drug resistance by affecting the tumor cell cycle. At present, many studies have reported that lncRNAs are involved in the drug resistance of PCa (25,26). Such as, lncRNA PCAT1 was found to promote the castration resistance of PCa patients by activating the AKT and NF-kappa B signaling pathway (27). Additionally, LncRNA HORAS5 promotes taxane resistance in castration-resistant PCa via a BCL2A1-dependent mechanism (28). LncRNA PCBP1-AS1-mediated AR/AR-V7 deubiquitination enhances PCa enzalutamide resistance (29). Previous studies have reported that lncRNA can regulate the function of downstream miRNA through the ceRNA mechanism, thus regulating the expression of target genes (12,30). Using bioinformatics software analysis, dual-luciferase reporter gene, and RNA pull-down assays, it was found that NONHSAT210528 binds to miR-21-5p, and regulates the function of miR-21-5p. Subsequently, using bioinformatics, dual-luciferase reporter gene, and RNA pull-down assays, we found that

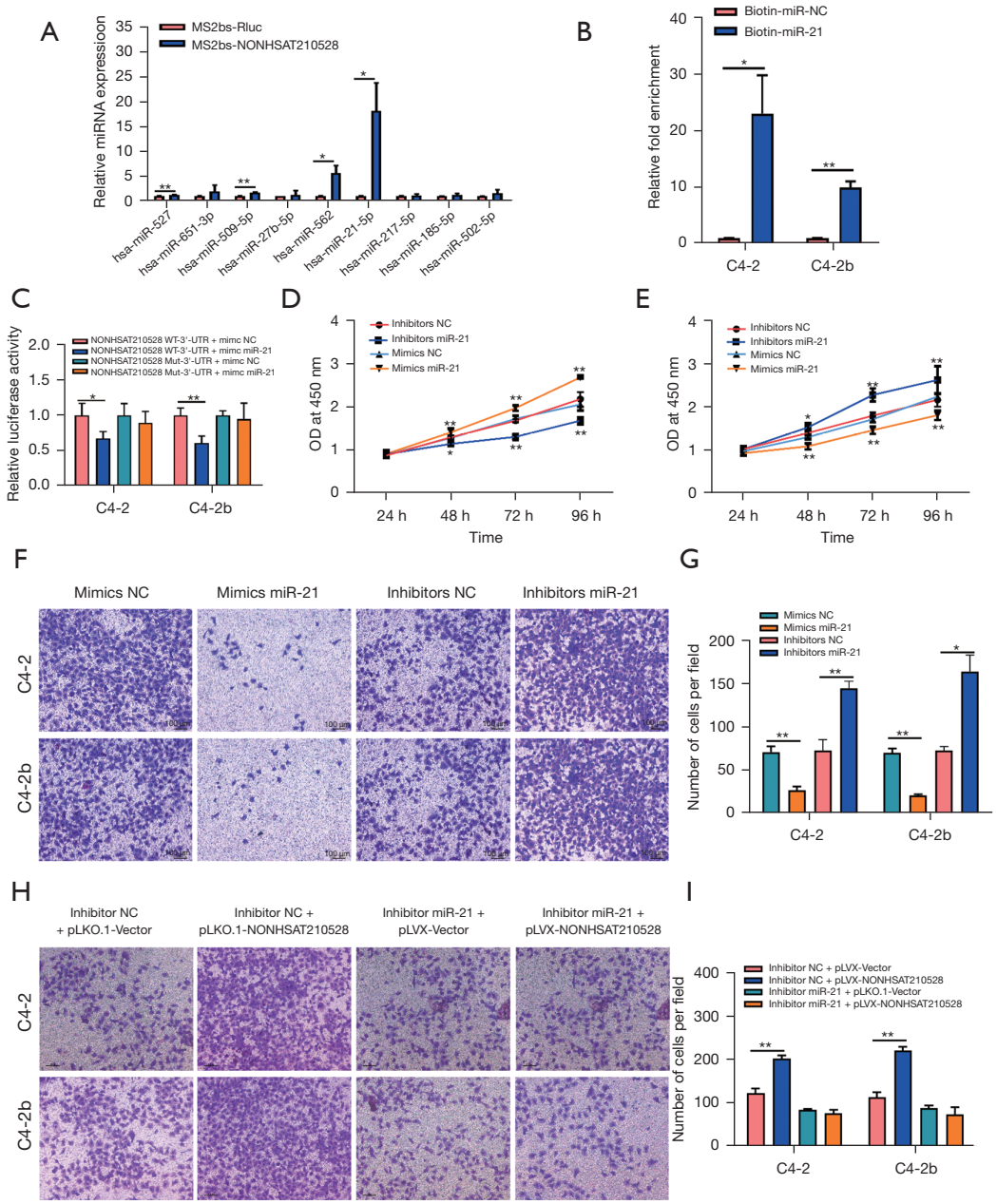

Figure 7 LncRNA NONHSAT210528 regulated the function of miR-21. (A) LncRNA NONHSAT210528 RNA pull down detected the combination of NONHSAT210528 and miRNA. (B) miR-21 RNA pull down detected the combination of NONHSAT210528 and miR-21. (C) Luciferase reporter gene analysis detected the combination of NONHSAT210528 and miR-21. (D) CCK-8 detected the proliferation of C4-2 cells with miR-21 overexpression or knockdown. (E) CCK-8 detected the proliferation of C4-2b cells with miR-21 overexpression or knockdown. (F) Transwell assays detected the invasion of C4-2 and C4-2b cells with miR-21 overexpression or knockdown. The cells at the bottom of the Transwell chambers were stained with crystal violet, scale bar, 100 μm. (G) Quantitative analysis of Transwell detection of the invasion of C4-2 and C4-2b cells with miR-21 overexpression or knockdown. (H) Transwell detection of the effect of NONHSAT210528 on the invasion of C4-2 and C4-2b cells with miR-21 knockdown. The cells at the bottom of the Transwell chambers were stained with crystal violet, scale bar, 100 μm. (I) Quantitative analysis of Transwell detection of the effect of NONHSAT210528 on the invasion of C4-2 and C4-2b cells with miR-21 knockdown. Scale bar, 100μm. *, P<0.05; **, P<0.01 compared to the control group. lncRNA, long non-coding RNA. OD, optical density.

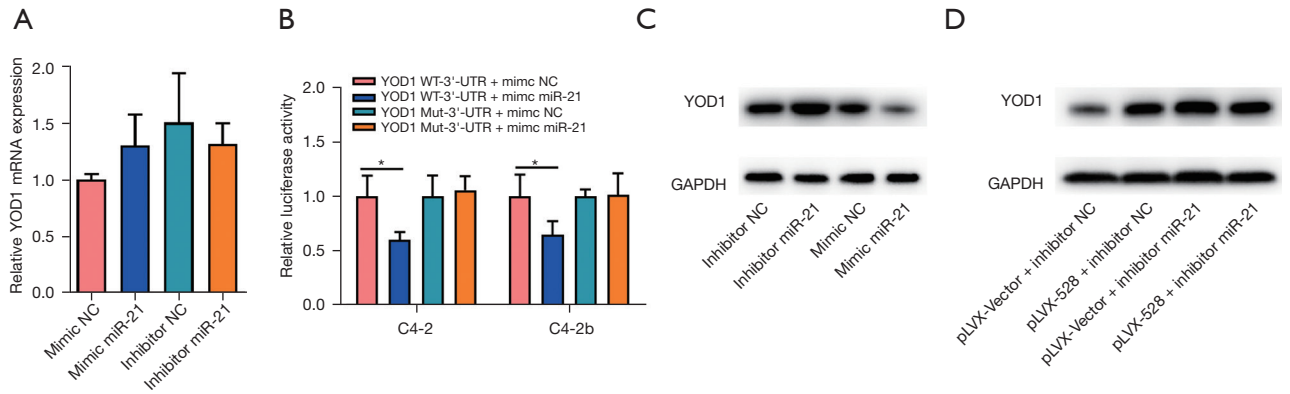

Figure 8 LncRNA NONHSAT210528 regulated the expression of YOD1 dependent on miR-21. (A) Real-time PCR detected YOD1 mRNA expression of C4-2 cells with miR-21 knockdown or overexpression. (B) Luciferase reporter gene analysis detected the combination of YOD1 3'-UTR and miR-21. (C) Western blot detected the YOD1 protein expression of C4-2 cells with miR-21 knockdown or overexpression. (D) Western blot detected the effect of NONHSAT210528 on the YOD1 protein expression with or without miR-21 knockdown. *, P<0.05 compared to the control group. lncRNA, long non-coding RNA; PCR, polymerase chain reaction.

miR-21-5p targets the expression of YOD1. YOD1 is a highly conserved deubiquitinase in the otubain family, which removes ubiquitin residues from polyubiquitinated proteins. Despite being highly conserved, the function of YOD1 in high-grade eukaryotes is not clear. YOD1, as a target gene of miR-4429, regulates the metastasis of ovarian cancer (31). LncRNA FIRRE promotes the progression of gallbladder cancer by mediating the expression of YOD1 through a ceRNA mechanism (32). It has been reported that YOD1 may become a biomarker for the prognostic evaluation of PCa (33). In this study, we found that YOD1 is involved in the resistance of enzalutamide, which may become a new target for the treatment of enzalutamide resistance.

Conclusions

Enzalutamide-resistant related lncRNA NONHSAT210528 appears to promote the proliferation and invasion of C4-2 and C4-2b cells by functioning as a ceRNA and regulating the miR-21-5p/YOD1 signal pathway.

Acknowledgments

Funding: This work was supported by the Changhai Hospital GCP platform (No. 2017ZX09304030) and Changhai Hospital Youth Start-Up Fund (No. 2019QNA02).

Footnote

Reporting Checklist: The authors have completed the ARRIVE reporting checklist. Available at https://tau.amegroups.com/article/view/10.21037/tau-22-99/rc

Data Sharing Statement: Available at https://tau.amegroups.com/article/view/10.21037/tau-22-99/dss

Conflicts of Interest: The author has completed the ICMJE uniform disclosure form (available at https://tau.amegroups.com/article/view/10.21037/tau-22-99/coif). The author has no conflicts of interest to declare.

Ethical Statement: The author is accountable for all aspects of the work in ensuring that questions related to the accuracy or integrity of any part of the work are appropriately investigated and resolved. Experiments were performed under a project license (No. 2019QN02) granted by Animal Care and Use Committee of Shanghai Changhai Hospital, the First Affiliated Hospital of Naval Military Medical University, in compliance with eighth edition guidelines for the care and use of experimental animals.

References

1. Torre LA, Bray F, Siegel RL, et al. Global cancer statistics, 2012. CA Cancer J Clin 2015;65:87-108.
2. Haffner MC, Zwart W, Roudier MP, et al. Genomic and phenotypic heterogeneity in prostate cancer. Nat Rev Urol 2021;18:79-92.
3. Chen W, Zheng R, Baade PD, et al. Cancer statistics in China, 2015. CA Cancer J Clin 2016;66:115-32.
4. Scher HI, Fizazi K, Saad F, et al. Increased survival with enzalutamide in prostate cancer after chemotherapy. N Engl J Med 2012;367:1187-97.
5. Annala M, Vandekerkhove G, Khalaf D, et al. Circulating Tumor DNA Genomics Correlate with Resistance to Abiraterone and Enzalutamide in Prostate Cancer. Cancer Discov 2018;8:444-57.
6. Li S, Fong KW, Gritsina G, et al. Activation of MAPK Signaling by CXCR7 Leads to Enzalutamide Resistance in Prostate Cancer. Cancer Res 2019;79:2580-92.
7. Chen WS, Aggarwal R, Zhang L, et al. Genomic Drivers of Poor Prognosis and Enzalutamide Resistance in Metastatic Castration-resistant Prostate Cancer. Eur Urol 2019;76:562-71.
8. Goodall GJ, Wickramasinghe VO. RNA in cancer. Nat Rev Cancer 2021;21:22-36.
9. McCabe EM, Rasmussen TP. lncRNA involvement in cancer stem cell function and epithelial-mesenchymal transitions. Semin Cancer Biol 2021;75:38-48.
10. Iaccarino I, Klapper W. LncRNA as Cancer Biomarkers. Methods Mol Biol 2021;2348:27-41.
11. Huarte M. The emerging role of lncRNAs in cancer. Nat Med 2015;21:1253-61.
12. Yuan JH, Yang F, Wang F, et al. A long noncoding RNA activated by TGF-β promotes the invasion-metastasis cascade in hepatocellular carcinoma. Cancer Cell 2014;25:666-81.
13. Prensner JR, Iyer MK, Sahu A, et al. The long noncoding RNA SChLAP1 promotes aggressive prostate cancer and antagonizes the SWI/SNF complex. Nat Genet 2013;45:1392-8.
14. Li C, Wang S, Xing Z, et al. A ROR1-HER3-lncRNA signalling axis modulates the Hippo-YAP pathway to regulate bone metastasis. Nat Cell Biol 2017;19:106-19.
15. Xiao G, Yao J, Kong D, et al. The Long Noncoding RNA TTTY15, Which Is Located on the Y Chromosome, Promotes Prostate Cancer Progression by Sponging let-7. Eur Urol 2019;76:315-26.
16. Liu C, Lou W, Zhu Y, et al. Niclosamide inhibits androgen receptor variants expression and overcomes enzalutamide resistance in castration-resistant prostate cancer. Clin Cancer Res 2014;20:3198-210.
17. Carbone L. Pain management standards in the eighth edition of the Guide for the Care and Use of Laboratory Animals. J Am Assoc Lab Anim Sci 2012;51:322-8.
18. Tannock IF, de Wit R, Berry WR, et al. Docetaxel plus prednisone or mitoxantrone plus prednisone for advanced prostate cancer. N Engl J Med 2004;351:1502-12.
19. Beer TM, Armstrong AJ, Rathkopf DE, et al. Enzalutamide in metastatic prostate cancer before chemotherapy. N Engl J Med 2014;371:424-33.
20. Maughan BL, Luber B, Nadal R, et al. Comparing Sequencing of Abiraterone and Enzalutamide in Men With Metastatic Castration-Resistant Prostate Cancer: A Retrospective Study. Prostate 2017;77:33-40.
21. Dong H, Hu J, Zou K, et al. Activation of LncRNA TINCR by H3K27 acetylation promotes Trastuzumab resistance and epithelial-mesenchymal transition by targeting MicroRNA-125b in breast Cancer. Mol Cancer 2019;18:3.
22. Zhou B, Yang H, Yang C, et al. Translation of noncoding RNAs and cancer. Cancer Lett 2021;497:89-99.
23. Kumar MM, Goyal R. LncRNA as a Therapeutic Target for Angiogenesis. Curr Top Med Chem 2017;17:1750-7.
24. Matsui M, Corey DR. Non-coding RNAs as drug targets. Nat Rev Drug Discov 2017;16:167-79.
25. Jiang X, Guo S, Zhang Y, et al. LncRNA NEAT1 promotes docetaxel resistance in prostate cancer by regulating ACSL4 via sponging miR-34a-5p and miR-204-5p. Cell Signal 2020;65:109422.
26. Ding L, Wang R, Shen D, et al. Role of noncoding RNA in drug resistance of prostate cancer. Cell Death Dis 2021;12:590.
27. Shang Z, Yu J, Sun L, et al. LncRNA PCAT1 activates AKT and NF-κB signaling in castration-resistant prostate cancer by regulating the PHLPP/FKBP51/IKKα complex. Nucleic Acids Res 2019;47:4211-25.
28. Pucci P, Venalainen E, Alborelli I, et al. LncRNA HORAS5 promotes taxane resistance in castration-resistant prostate cancer via a BCL2A1-dependent

mechanism. Epigenomics 2020;12:1123-38.
29. Zhang B, Zhang M, Shen C, et al. LncRNA PCBP1-AS1-mediated AR/AR-V7 deubiquitination enhances prostate cancer enzalutamide resistance. Cell Death Dis 2021;12:856.
30. Qi X, Zhang DH, Wu N, et al. ceRNA in cancer: possible functions and clinical implications. J Med Genet 2015;52:710-8.
31. Zhu YM, Chen P, Shi L, et al. MiR-4429 suppresses the malignant development of ovarian cancer by targeting YOD1. Eur Rev Med Pharmacol Sci 2020;24:8722-30.
32. Wang S, Wang Y, Wang S, et al. Long Non-coding RNA FIRRE Acts as a miR-520a-3p Sponge to Promote Gallbladder Cancer Progression via Mediating YOD1 Expression. Front Genet 2021;12:674653.
33. Ciszkowicz E, Porzycki P, Semik M, et al. MiR-93/miR-375: Diagnostic Potential, Aggressiveness Correlation and Common Target Genes in Prostate Cancer. Int J Mol Sci 2020;21:5667.

Cite this article as: Ye C, Chen YG, Qin SF, Tang SY, Li S, Shi MF, Zhou T. Enzalutamide-resistant related lncRNA NONHSAT210528 promotes the proliferation and invasion of prostate cancer. Transl Androl Urol 2022;11(5):643-658. doi: 10.21037/tau-22-99

